Modeling of the Space Shuttle Solid Rocket Motor Nozzle Boot Cavity Pressurization Process

J. Louie Clayton*
United Technologies, USBI, Huntsville, Alabama

Pressurization of the Space Shuttle solid rocket motor (SRM) nozzle boot cavity involves compressible gas flow along a duct with friction and a pressurizing volume with heat transfer at the boundaries. Numerical simulation of the process requires a solution of the simultaneous compressible flow, boot cavity conservation, and solid-conduction equations. Basic geometry consists of circular flow path connected to a plenum-free volume that is surrounded by a solid-conduction media (i.e., the cowl vent holes, boot cavity, and cavity insulation). An existing methodology is used to compute the compressible mass-flow rates through the vent hole. Boot cavity conditions are computed by the application of a finite-difference form of the conservation equations. In the boot cavity insulation (i.e., the solid-conduction regions), the finite-difference transient diffusion equation is applied. A conjugate solution is developed whereby the coupled first-order differential equations are solved simultaneously, along with a set of algebraic equations, by fully implicit successive point iteration. A model was constructed to simulate a boot cavity pressurization test, and a comparison of model response vs test data is given. The agreement is generally good.

Nomenclature

A = area
B = backwards time difference
C = thermal capacitance
C-N = Crank-Nicholson
C_g = combustion gas specific heat/time step
C_i = insulation specific heat/time step
C_p = gas specific heat, constant pressure
C_v = gas specific heat, constant volume
DM-9 = solid rocket motor development model-9
DTIME = program time step
F = forward time difference
G_c = cavity gas conductor (molecular conduction)
G_{ij} = insulation conductor
G_r = cavity gas radiation conductor
g = gravitational constant
h = enthalpy
$k(T,P)$ = gas thermal conductivity, pressure- and temperature-dependent
k_i = insulation thermal conductivity
ℓ = cavity gas optical thickness
l/d = flow path length/diameter
M = mixture molecular weight
MAX = maximum number of loops
m = total mass of gas in cavity
$\dot{m}$ = mass-flow rate
m_a = mass of air in cavity
m_g = mass of combustion gas in cavity
NNT = total number of thermal nodes
OBR = outer boot ring
OUT = simulation output time
P = pressure
$\dot{Q}_c$ = conduction heat-transfer rate
$\dot{Q}_r$ = radiation heat-transfer rate
$\dot{Q}_t$ = total heat-transfer rate at cavity boundary $(\dot{Q}_r + \dot{Q}_c)$
$\bar{R}$ = universal gas constant
$RLXC$ = largest computed residual
T = temperature
TIME = simulation time
TOL = relaxation tolerance
T_b = bulk gas temperature
T = insulation temperature
T_w = cavity wall temperature
u = cavity gas internal energy
α = insulation thermal diffusivity
Δt = time increment
Δx = conduction path length
ε_F = radiative gray body factor
ε_g = total hemispherical gas emissivity
ε_w = total hemispherical wall emissivity
ρ = gas density
σ = Stefan-Boltzmann constant
ϕ = constant based on percent aluminum oxide in propellant gas

Subscripts

a = air
b = bulk
c = conduction
F = form factor derived
g = gas
i = insulation
ij = connecting nodes i and j
in = inlet
j = free index used for arbitrary nodes
o = outlet
p = constant pressure
r = radiation
t = total quantity
v = constant volume
w = wall

Superscripts

o = stagnation conditions
$'$ = (prime) evaluated at end of time step

Received Oct. 3, 1988; revision received Dec. 27, 1988.

*Senior Analytical Engineer.

Introduction

THE nozzle of the Space Shuttle solid rocket motor (SRM) provides for thrust vectoring by mounting the assembly to a flexible bearing that is fixed to the aft end of the SRM

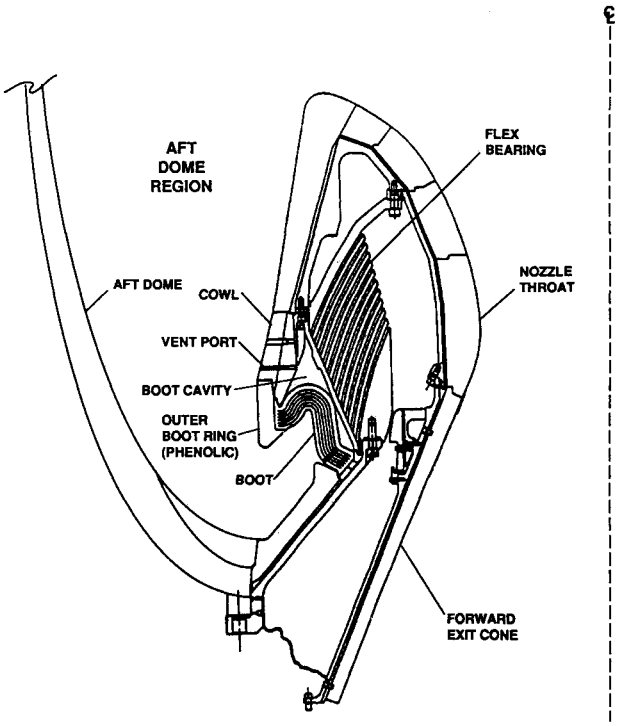

Fig. 1 SRM nozzle cross section showing flex-bearing and boot cavity.

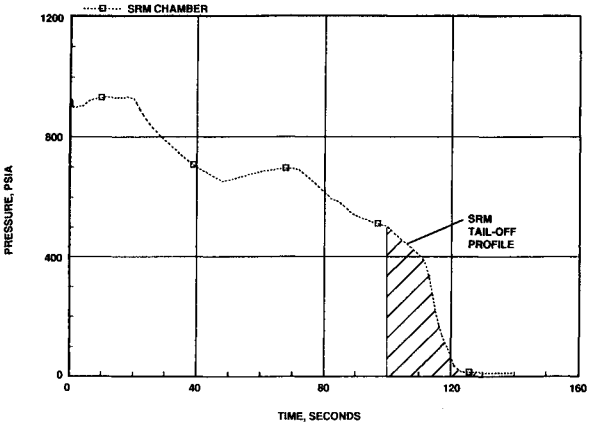

Fig. 2 Typical SRM chamber pressure trace.

motor case. The "flex"-bearing structure (Fig. 1) is protected from internal motor environments by a flexible boot. A free volume exists between the boot and flex-bearing assembly, which is vented to the aft dome region of the SRM. During the SRM motor ignition transient, when chamber conditions are building to flight pressure and temperature, the free volume behind the boot is pressurized through the vent holes. This process first occurs by pressurization with cold air that is local to the aft dome, and then by hot combustion gases. A condensable metallic component (aluminum oxide) is present in the combustion gas. During the pressurization process, the aluminum oxides have a tendency to condense out of the combustion gases on the flow path, thus restricting flow into or out of the boot cavity.

During a recent SRM static test firing (designated DM-9 SRM), a failure of the nozzle outer boot ring occurred. Segments of the phenolic material (Fig. 1) had fractured and separated from the boot assembly. The cause of the failure was thought to be due in part to a negative pressure differential across the outer boot ring.

The pressure inside the boot cavity at some time during the motor burn was higher than the pressure in the aft dome region. It was determined by use of models that this condition could only occur when the solid propellant was almost ex-

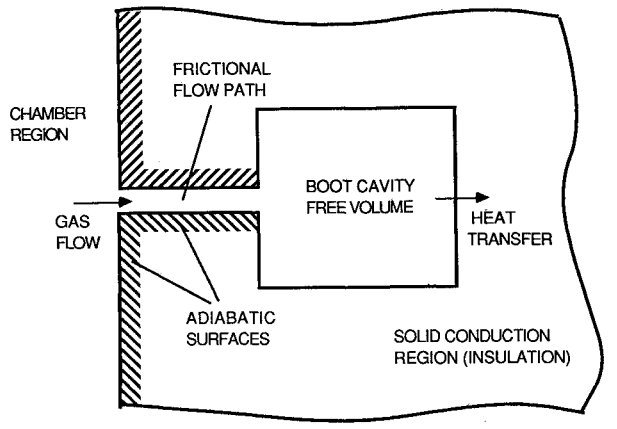

Fig. 3 Simplified boot cavity model geometry.

pended and the pressure profile (Fig. 2) was "tailing." At this time, if the vent holes were clogged due to condensation of aluminum oxide, a considerable negative pressure differential could exist across the outer boot ring assembly.

A series of subscale vent hole-boot cavity pressurization tests[1] were conducted at Marshall Space Flight Center (MSFC). The objectives of these tests were to 1) investigate the condensation buildup characteristics of the baseline vent design, 2) access the performance of alternate vent designs, and 3) provide data for the calibration of numerical math models. During the first test, the vent hole was plugged by aluminum oxide. Inspection of the data revealed that most of the vent closure occurred at about 15–25 s into the test. This fact was indicated by an abrupt deviation between the chamber and boot cavity pressure trace data. An observable characteristic in the cavity pressure trace, after 20 s, is an asymptotic cooling profile. This is indicative of a flow decoupling from the chamber (i.e., vent holes were essentially blocked, and cooling was occurring by heat transfer to the cavity walls).

Using the methodology that is given in the following sections, the MSFC boot cavity pressurization test was modeled. A comparison of model response vs test data is given.

Development of Basic Equations

The total volume of the flight vehicle nozzle boot cavity is approximately 3348 in.[3] and is vented by 36 vent holes that are evenly spaced around the circumference of the cowl assembly. To simplify the problem solution, only one vent hole is considered, and 1/36 of the total cavity volume is used. A schematic of the simplified boot cavity model geometry is shown in Fig. 3.

Bulk Gas Energy Equation

Conservation of energy in the boot cavity free volume is developed using the time-dependent uniform-state, uniform-flow energy equation.[2] Expressed as a rate equation, it is given as

$$\dot{Q}_t + \dot{m}_{\text{in}} h_{\text{in}} = \frac{d}{dt}(mu) + \dot{m}_o h_o \qquad (1)$$

Several basic assumptions are associated with the use of this equation. 1) The contents of the boot cavity exist at a uniform temperature, pressure, and composition. 2) No mechanical work occurs at the boundaries of the cavity. 3) The gas enthalpy entering or leaving the cavity is uniform over the flow area. 4) Potential energy terms are negligible. 5) Vent hole exit stagnation enthalpy is used as the inlet flow enthalpy to the cavity. 6) The filling process occurs at constant volume.

Cavity Heat Transfer by Radiation

The first term in Eq. (1) is the cavity heat-loss rate. In this study, this term comprises two components: stagnant gas

conduction and radiation. When the cavity is pressurizing with cold air, the radiation contributions are small because the boot cavity temperatures are relatively cool, the boot cavity is small, and the air is optically thin.

When the cavity is pressurizing with hot gas (i.e., after cold-air pressurization), the overall bulk gas temperature response in the cavity is not influenced to any extent by radiation (or convection) to the cavity walls. The reason for this effect is that the convected energy through the vent hole and into the cavity is much larger in magnitude than any of the other contributors to the energy balance.

When pressurization of the cavity is complete, the convected enthalpy rates are essentially zero, bulk gas temperatures are hot, and metallic oxides are present in the boot cavity gas. The radiation heat-transfer rate from the cavity gas to the insulation is significant.

The net rate of radiation heat loss by the gas to the cavity wall is

$$\dot{Q}_r = \sigma A \varepsilon_F (T_w^4 - T_b^4) \tag{2}$$

The diffuse "gray body" factor contained in Eq. (2) is computed as follows. The combustion gas emissivity is expressed as a function of gas density, percentage of aluminum oxide, and cavity gas optical thickness. The basic correlation used in the model[3] is

$$\varepsilon_g = 1 - e^{-\phi \rho \ell} \tag{3}$$

The cavity gas optical thickness is taken to be the average distance across the cavity volume. The gas density contained in Eq. (3) is computed using the ideal gas equation of state evaluated at bulk cavity conditions. If the cavity is pressurizing with air, then the percentage term in Eq. (3) is set to approximately zero.

The gas-to-wall effective gray body factor is calculated using the expression developed for radiative exchange between infinite parallel flat plates

$$\varepsilon_F = 1 \Big/ \left(\frac{1}{\varepsilon_w} + \frac{1}{\varepsilon_g} - 1 \right) \tag{4}$$

Since radiation heat-transfer rates are quartic in absolute temperature, Eq. (2) cannot be readily cast into a format that is compatible with the numerical solution routine. This term is expanded by the standard linearization formula

$$\dot{Q}_r = G_r (T_w - T_b) \tag{5}$$

where

$$G_r = \sigma A \varepsilon_F (T_b^2 + T_w^2)(T_b + T_w)$$

The rate of radiation heat transfer is now expressed as a function of the simple temperature difference times a nonlinear coefficient. This formulation allows the bulk gas temperature to be algebraically factored with other bulk gas temperature terms that result in the energy equation. The temperature-dependent coefficient now becomes a term that can be converged by iteration.

Cavity Heat Transfer by Gas Conduction

In conjunction with gas radiation, heat transfer between the gas and wall is occurring by molecular conduction. During the pressurization process, when cavity turbulence is high, the bulk gas temperature is primarily driven by the convected energy entering through the vent hole. Thus forced convection to the cavity walls is present, but has little influence on the magnitude of the bulk gas temperatures. After the boot cavity has been pressurized, gas velocities in the cavity are negligible, and forced convection reduces to stagnant gas conduction. The rate of heat transfer due to stagnant gas conduction is

$$\dot{Q}_c = G_c (T_w - T_b) \tag{6}$$

where

$$G_c = \frac{k(T,P)A}{\Delta x}$$

The gas conductivity in Eq. (6) depends on temperature and boot cavity pressure. The temperature dependency is evaluated at gas-to-wall film conditions. The heat-flow path length is taken as an average distance from the geometric center of the cavity to the cavity walls. The nonlinearity presented by the temperature and pressure-dependent conductivity is treated numerically as is the nonlinear radiation coefficient contained in Eq. (5).

The total cavity heat-loss rate contained in Eq. (1) is given by the sum of Eqs. (5) and (6). The two modes of heat transfer are assumed to act in parallel and independently of each other and are sufficient to approximately quantify the total rates of heat transfer from the bulk gas to the cavity walls.

Cavity Energy Storage and Gas Enthalpy Terms

When pressurizing the boot cavity, the mass of gas in the cavity changes with time, and the internal energy of the gas also changes with time. Thus, expanding the derivative in the storage term of Eq. (1), applying the continuity equation, and using ideal-gas approximations, the storage term now takes the following form:

$$\frac{d}{dt}(mu) = mC_v \frac{dT_b}{dt} + C_v T_b (\dot{m}_{\text{in}} - \dot{m}_o) \tag{7}$$

Ideal-gas approximations are also used to compute the enthalpy into and out of the cavity. Stagnation enthalpy for Fanno flow is constant. Using this assumption, the total flow energy (enthalpy + kinetic) that enters the boot cavity is equal to the stagnation enthalpy at the entrance to the vent hole. When flow occurs out of the cavity, the enthalpy of the exit stream is evaluated at the bulk gas temperature and composition. The boot cavity gas enthalpy terms are approximated by

$$\dot{m}_{\text{in}} h_{\text{in}} = \dot{m}_{\text{in}} C_p T_{\text{in}}^o \tag{8a}$$

$$\dot{m}_o h_o = \dot{m}_o C_p T_b \tag{8b}$$

Combining terms that have been expanded in Eqs. (2–8) and solving for the bulk gas differential term, the first-order nonlinear differential equation is obtained:

$$mC_v \frac{dT_b}{dt} = C_v T_b (\dot{m}_o - \dot{m}_{\text{in}}) + \dot{m}_{\text{in}} C_p T_{\text{in}}^o - \dot{m}_o C_p T_b + \dot{Q}_t \tag{9}$$

Cavity Mass Balance

During the SRM ignition transient, filling of the boot cavity initially occurs with cold air. This is followed by filling with hot combustion products. The boot cavity conservation of mass equation is developed for the two components. Combustion gas properties[4] are tabulated as quantities of a gas of equivalent molecular weight. The tabulated properties for air and combustion gas are then used to determine overall mixture properties in the cavity based on computed mass fractions. No recombination of air and combustion gas is permitted. The constituency of the cavity gas is determined only by the relative proportions of gas that flow into the cavity through the vent hole.

The cavity mass balance equations for the two components are

$$\frac{dm_g}{dt} = (\dot{m}_{\text{in}} - \dot{m}_o)_g \tag{10a}$$

$$\frac{dm_a}{dt} = (\dot{m}_{\text{in}} - \dot{m}_o)_a \tag{10b}$$

$$m = m_g + m_a \tag{10c}$$

Vent Hole Mass Flow Rate

During boot cavity pressurization, gas flows through 0.31-in.-diam vent holes and into the boot cavity. The flow-path cross section is circular, and the flow-path length is approximately 3.7 in. long. Because of the l/d of the flow path, frictional effects are considered in the calculation of mass-flow rates. The flow is also treated as compressible. This leads tp an approach developed by Lapple[5] that considers compressible flow with friction in a constant-area duct. The Fanno relationships have been modified to include the influence of an entrance and then integrated over a fixed path length. Mass-flow rates are calculable as a tabulated function of entrance/exit conditions, friction, and the flow-path l/d.

The procedure, first of all, requires the calculation of an isothermal mass-flow rate that is given by the following relationship:

$$\dot{m} = PA\sqrt{\frac{M_g}{eRT}} \tag{11}$$

Pressure, temperature, and molecular weight terms contained in this equation are evaluated at "upstream" conditions. Equation (11) is modified by a factor that is a function of flow-path friction and the two independent variables flow-path l/d and the ratio of entrance-to-exit pressures.

The friction factor is calculated as a function of the average flow-path Reynolds number using standard relationships derived for rough surface circular ducts. Laminar-to-turbulent transition is assumed to occur at a Reynolds number of 2000.

Using Eq. (11) and tabulated flow factors,[5] calculation of compressible mass flow rates through the vent hole is reduced to the explicit evaluation of a few algebraic equations. These equations are easily incorporated into the overall numerical solution.

Solid Conduction into the Cavity Walls

In the solid regions (i.e., the boot cavity insulation), heat flow is assumed to be one dimensional and is described by the transient diffusion equation

$$\frac{\partial T}{\partial t} = \alpha\frac{\partial^2 T}{\partial x^2} \tag{12}$$

A solution to Eq. (12) is achieved by a lumped parameter (R-C network) formulation. Boundary conditions between the cavity gas and the wall insulation are provided in the following section.

Boundary Conditions

The boundary conditions that initially drive the model responses are defined by the combustion gas properties local to the vent hole inlet. For the SRM and subscale motors, these quantities are approximately known and usually expressed as functions of time. Because of the impingement characteristics of the flowfield in the aft dome region of the SRM, stagnation properties are used.

Assuming that there is no ablation of the boot cavity wall insulation, heat-transfer rates at the wall are described by the following "surface" boundary condition:

$$k_i\frac{dT_w}{dx} = G_r(T_b - T_w) + G_c(T_b - T_w) \tag{13}$$

The assumption of no ablation appears to be valid based on the observed physical condition of the surfaces inside the boot cavity. Typically the insulations inside the cavity show no sign of ablation and are affected very little by heat.

No "backside" heating conditions are used in modeling the solid conduction portions of the boot cavity model. Rather, the network is allowed to become computationally adiabatic in the direction of heat transfer (i.e., negligible temperature difference between successive nodes). This is equivalent to solid conduction into a semi-infinite slab.

Finite Differencing the Conservation Equations

The bulk gas energy differential equation (9) is finite differenced in time by the Crank-Nicolson (C-N) method. The basic format is

$$C\frac{\Delta T_b}{\Delta t} = \frac{1}{2}(F + B) \tag{14}$$

All dependent variables involved with the forward time difference are evaluated once at the beginning of the time step. Combining terms for the forward time difference gives

$$F = C_v T_b(\dot{m}_o - \dot{m}_{\text{in}}) + \dot{m}_{\text{in}} C_p T^o_{\text{in}} - \dot{m}_o C_p T_b$$

$$+ G_r(T_w - T_b) + G_c(T_w - T_b)$$

Dependent variables occurring in the backward time difference are solved by iteration for a given time step. Their values are denoted by a prime. Combining the forward and backward terms by plugging into Eq. (14) and solving for the primed bulk gas temperature term gives

$$T'_b = \frac{2\bar{C}_g T_b + F + \dot{m}_{\text{in}} C_p T'^o_{\text{in}} + (G_r + G_c)T'_w}{2\bar{C}_g + \dot{m}_o(C_p - C_v) + \dot{m}_{\text{in}} C_v + G_r + G_c} \tag{15}$$

This is the final form of the bulk gas energy equation used in the numerical procedure. The equation as formulated is implicit and is solved by the algorithm provided in the following section.

The conservation of mass equations are solved by the implicit modified Euler method. Basic forms of the finite-difference equations are

$$m'_g = m_g + \frac{\Delta t}{2}[(\dot{m}_{\text{in}} - \dot{m}_o)'_g + (\dot{m}_{\text{in}} - \dot{m}_o)_g] \tag{16a}$$

$$m'_a = m_a + \frac{\Delta t}{2}[(\dot{m}_{\text{in}} - \dot{m}_o)'_a + (\dot{m}_{\text{in}} - \dot{m}_o)_a] \tag{16b}$$

$$m' = m'_g + m'_a \tag{16c}$$

The predictor evaluation of the mass-flow rate occurs at the beginning of the time step based on the current values of the dependent variables. The corrector mass-flow rate evaluation (i.e., the primed quantities) is determined by inclusion of the calculation in the iterative loop. This procedure is then marched in time to obtain a transient solution.

Evaluation of the ideal-gas equation of state occurs at the beginning of the time step and is also included in the corrector iteration procedure. The equation of state provides the computation of cavity pressure based on the three dependent variables: 1) total mass of gas in the cavity, 2) bulk gas temperature, and 3) gas mixture molecular weight.

Neglecting source terms and finite differencing by the C-N method, the transient diffusion equation takes the following form:

$$T'_i = \frac{2\bar{C}_i T_i + \Sigma G_{ij}(T_j - T_i) + \Sigma G_{ij} T'_j}{2\bar{C}_i + \Sigma G_{ij}} \tag{17}$$

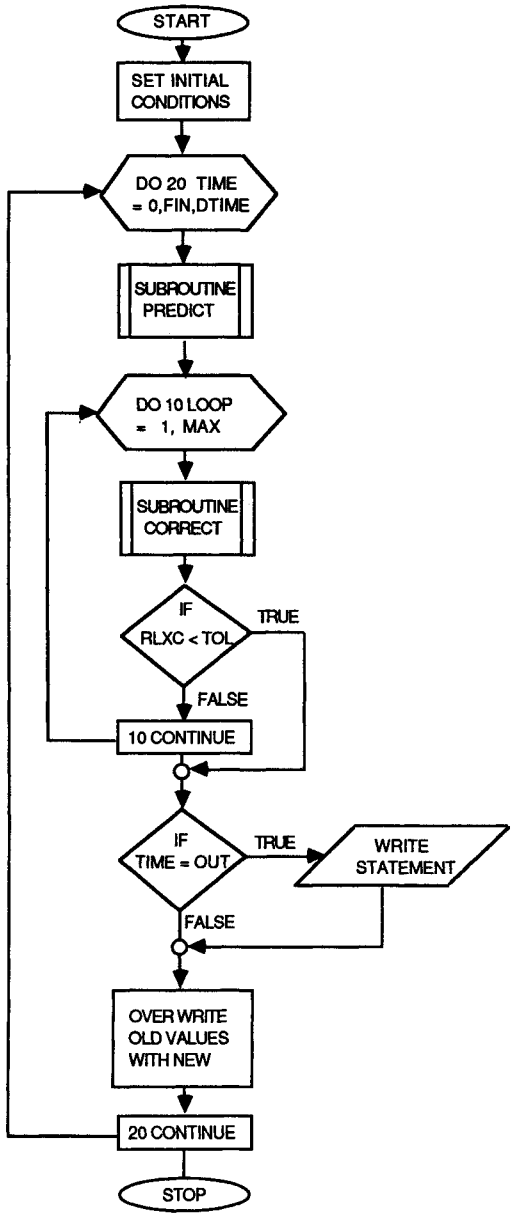

Fig. 4 Solution routine flowchart, driver segment.

The outermost cavity wall node is subjected to the boundary conditions that describe heat transfer from the gas to the solid-conduction regions. In finite-difference form, the wall node steady-state energy equation is given as

$$T_w = \frac{G_{ij}T_i + G_rT_b + G_cT_b}{G_{ij} + G_r + G_c} \tag{18}$$

Numerical Solution

The finite-difference equations developed in the previous section are solved by a successive point, partial back substitution technique. The calculation procedure implicitly solves both the bulk gas and solid-conduction domains simultaneously (i.e., a conjugate solution is performed). All nonlinearities in the dependent variables of integration are dealt with by iteration. A slight amount of damping (about 5%) is used. Because heavy damping is not required, relaxation checking is performed by capturing and evaluating the temperature, pressure, and mass residuals over successive iterations. Given the uncertainties in the boundary values, geometry, etc., residuals of 1% give sufficiently accurate results.

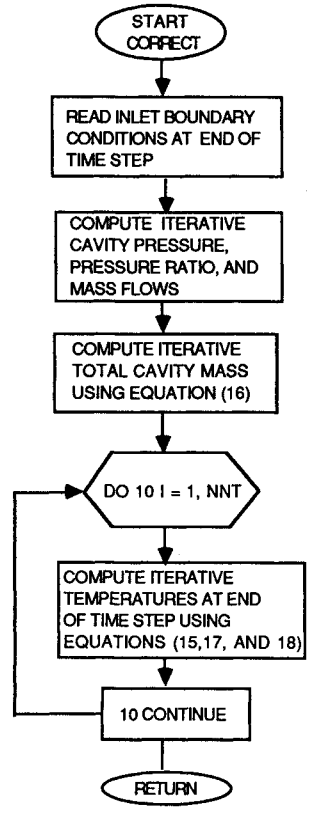

Fig. 5 Solution routine flowchart, subroutine correct.

To provide a concise picture of the algorithm, a flow chart of the FORTRAN calculation procedure is given in Figs. 4–6. Arithmetic steps, conditionals, and transfers are denoted using standard flowchart terminology. Equation numbers used in the arithmetic steps correspond to the numbering scheme established in this study.

The algorithm starts by setting up initial conditions. Execution then branches to subroutine PREDICT where, first, inlet pressure and temperature interpolations are performed, then the ideal-gas equation is evaluated with the current values of temperature and cavity mass. Next, based on the conditions at the beginning of the time step, the cavity mass predict derivative is evaluated (i.e., calculation of compressible mass-flow rates). The forward time difference heat-transfer rates are calculated and stored. The iterative segment of the procedure is performed next. Execution falls into the inner loop (see Fig. 4) where the subroutine CORRECT is called. All dependent variables (temperatures and cavity mass) are iteratively evaluated at the end of time step using partial back substitution. The cavity mass correct derivative evaluation occurs using the iterative values of the dependent variables. The cavity pressure is updated each iteration, and a bulk gas temperature is calculated. The residuals in the primary variables are captured for each iteration and compared to the relaxation tolerance to determine if the solution for the given time step is adequately converged. If so, the following operations are performed: 1) the output interval is checked, 2) time is incremented, 3) overwrite the old dependent variables with the newly calculated ones, and 4) check for end of simulation time. If the problem stop time has not been reached, then solution routine execution branches back to subroutine PREDICT and continues with the next time step.

Modeling the MSFC Subscale Boot Cavity Test

The following section provides a discussion of a model that was constructed for the simulation of the MSFC subscale boot cavity pressurization tests. Vent hole diameter, flow-path

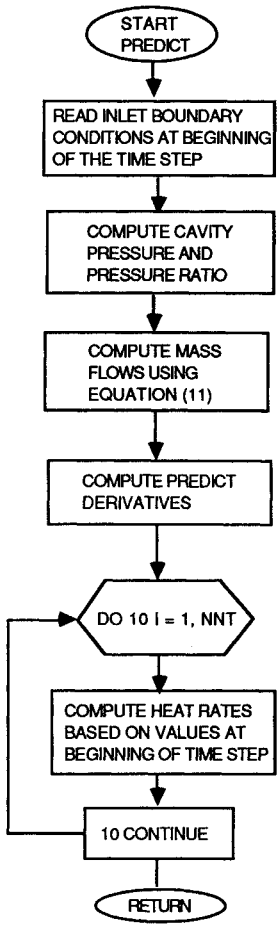

Fig. 6 Solution routine flowchart, subroutine predict.

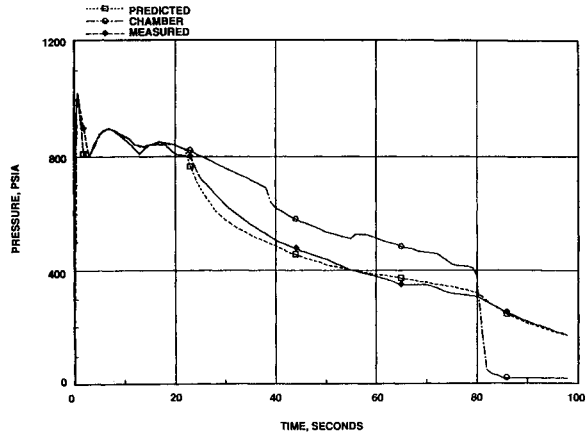

Fig. 7 Comparison of pressure trace data.

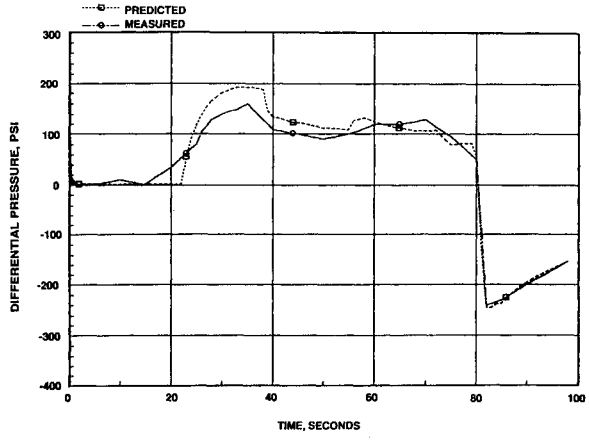

Fig. 8 Comparison of cowl differential pressure trace data.

length, and cavity fill volumes are approximately equivalent to SRM flight hardware. The computational procedure developed in this study was applied to the specific geometry and boundary conditions of the test.

Measured chamber conditions from the simulated boot cavity test provided the vent hole inlet thermal boundary conditions. The chamber pressure profile obtained from the first test is shown in Fig. 7. The chamber temperature measurement was saturated at 4100°F. It is known from similar tests that chamber temperatures are approximately 4300°F. Thus, the vent hole inlet temperatures were fixed at this temperature. Inlet gas properties are calculated as follows. If the simulation time is less than 100 ms, then local air temperatures and standard air compositions are used. If the simulation time is greater than 100 ms, then the vent hole inlet temperature is fixed at the measured gas temperature, and combustion gas mixture compositions are used. Switching of the inlet gas properties at 100 ms is based on the indicated time offset that occurs between the ignitor firing command and first indication of temperature sensor response at the test location in the motor.

For comparison purposes, a simple approach to vent hole blockage is used. The flow area is recomputed to be 0.15% of the original flow area at 22 s simulation time. This amount of flow blockage was determined to give the best fit of model response to the observed test data. The time of the blockage event (i.e., about 22 s) was chosen by visual inspection of the test data.

A minor modification was made to the governing equations to simulate a cavity bleed flow to ambient conditions. To test the condensation characteristics of the aluminum oxides in the vent hole, a 12-mil-diam orifice vents the simulated boot cavity to the atmosphere. This ensures that, after pressurization, a continuous flow occurs through the vent hole for the duration of the test. Mass-flow rates through the orifice were calculated using the equations developed by Lapple with the l/d fixed at zero.

Measured and predicted pressures for the boot cavity test are shown in Figs. 7 and 8. As indicated, agreement between model response and test data is generally good.

Conclusions

The model developed in this study was used to make a conservative estimate of the maximum expected differential pressure that could possibly occur across the flight SRM nozzle outer boot ring. This analysis was performed by assuming that the vent holes are completely plugged by aluminum oxides during SRM tailoff.

Improvements to the given methodology might include 1) effects of chemical recombination of air and combustion gases in the boot cavity, 2) inclusion of a simplified vent hole plugging model, and 3) simulation of boot cavity volume changes with time.

References

[1]"Nozzle Cowl Vent Port Plugging Test," Morton Thiokol, Thermal Analysis Group, Huntsville, AL, SRM-D-MSFC 3-18, May 1988.

[2]Van Wylen, G. and Sontag, R., "The Uniform-State, Uniform-Flow Process," *Introduction to Thermodynamics: Classical and Statistical*, Wiley, New York, 1971.

[3]"Aerothermal Analysis of the High Performance SRM Nozzle," Morton Thiokol, Heat Transfer and Gas Dynamic Sections, Wasatch, UT, TWR-14633, Jan. 1985.

[4]Whitesides, R. H., "SRM Thermochemical Data for TP-H1148 Propellant, Temperature and Pressure Specified," Spectra Research System (SRS) Technologies, Huntsville, AL, July 1986.

[5]Lapple, C. E., "Isothermal and Adiabatic Flow of Compressible Fluids," *Transcripts from American Institute of Chemical Engineers*, Vol. 39, 1943, pp. 385–432.